



Molecular dynamics simulation of the interaction between protein tyrosine phosphatase 1B and aryl diketoacid derivatives

Qiang Wang^{a,b}, Jun Gao^{a,b,*}, Yongjun Liu^a, Chengbu Liu^{a,**}

^a Key Laboratory of Colloid and Interface Chemistry, Ministry of Education, Institute of Theoretical Chemistry, School of Chemistry & Chemical Engineering, Shandong University, Jinan 250100, PR China

^b Key Laboratory of Theoretical and Computational Chemistry in Universities of Shandong (Shandong University), Jinan 250100, PR China

ARTICLE INFO

Article history:

Accepted 28 June 2012

Available online 7 July 2012

Keywords:

Protein tyrosine phosphatase 1B
Aryl diketoacids
Molecular dynamics simulation
Cooperative effect
Binding model

ABSTRACT

The protein tyrosine phosphatase 1B (PTP-1B) is acknowledged as an outstanding therapeutic target for the treatment of diabetes, obesity and cancer. In this work, six aryl diketoacid compounds have been studied on the basis of molecular dynamics simulations. Hydrogen bonds, binding energies and conformation changes of the WPD loop have been analyzed. The results indicated that their activation model falls into two parts: the target region of the monomeric aryl diketoacid compounds is the active site, whereas the target region of the dimeric aryl diketoacid compounds is the WPD loop or the R loop. The van der Waals interactions exhibit stronger effects than the short-range electrostatic interactions. The van der Waals interaction energy and the IC₅₀ values exhibit an approximately exponential relationship. Furthermore, the van der Waals interactions cooperate with the hydrogen bond interactions. This study provides a more thorough understanding of the PTP-1B inhibitor binding processes.

© 2012 Elsevier Inc. All rights reserved.

1. Introduction

Protein tyrosine phosphatases (PTPs) are a large family of enzymes that catalyze the conversion of phosphorylated tyrosine of protein into tyrosine and inorganic phosphate [1]. PTPs play an important role in biological processes, and they are a crucial modulator in the range of cellular processes such as cell growth, differentiation and metabolism [2–4]. Among PTPs, protein tyrosine phosphatase 1B (PTP-1B) has been found to be a negative regulator in both insulin and leptin signaling [5,6]. For example, PTP-1B-deficient mice display enhanced insulin sensitivity and improved glycemic control and resistance to a high-fat diet, which induces obesity [7,8]. Therefore, PTP-1B inhibitors have been considered as a promising drug candidate for the treatment of Type II diabetes, insulin resistance and obesity [9–12].

PTP-1B contains N-terminal and C-terminal domains. The N-terminal domain contains catalytic regions [13]. The C-terminal domain contributes to the location of the enzyme at the cytoplasmic face of the endoplasmic reticulum and influences the N-terminal domain by causing a global conformational change of PTP-1B

molecules that allows the formation of direct contacts between the catalytic domain and the phosphorylated substrates [14]. Interestingly, the catalytic domain contains two aryl phosphate-binding sites: a highly conserved active site (His214–Arg221) and a lowly conserved non-catalytic site B (Arg24 and Arg254) (Fig. 1), which is located adjacent to the active site [15]. In general, the most efficient inhibition is accomplished when the inhibitor occupies the active site. Therefore, the inhibitor should possess polar groups and be anionically charged at physiologic pH. At the same time, the inhibitor molecule is stably anchored through the formation of hydrogen bonds between particular amino acid residues and the functional groups of inhibitors within the active site. However, the polar groups will reduce the ability of the PTP-1B inhibitors to cross the cell membrane and access the cytosolic PTP-1B [16].

The WPD loop plays a role in the specificity and the affinity of the inhibitor. WPD (Thr177–Pro185) and R (Val113–Ser118) loops cover the active site when the inhibitor binds to the substrate. In the native form, no inhibitor binds to the PTP-1B; the WPD loop is in an open conformation, and the active site is easily accessible to the substrate. When the inhibitor is bound with the active site, the WPD loop closes over the active site, and the WPD loop and the active site subsequently form a tightly binding pocket for the substrate. To be specific for PTP-1B, the inhibitor should reduce the mobility of the WPD loop toward a more rigid conformation, which inhibits the closure of the WPD loop and prevents the substrate from binding [17,18]. Unfortunately, the discovered inhibitors exhibit poor selectivity toward PTP-1B.

* Corresponding author at: Key Laboratory of Colloid and Interface Chemistry, Ministry of Education, Institute of Theoretical Chemistry, School of Chemistry & Chemical Engineering, Shandong University, Jinan 250100, PR China.
Tel.: +86 531 88363967; fax: +86 531 88564464.

** Corresponding author. Tel.: +86 531 88361398; fax: +86 531 88564464.
E-mail addresses: gaojun@sdu.edu.cn (J. Gao), cbliu@sdu.edu.cn (C. Liu).

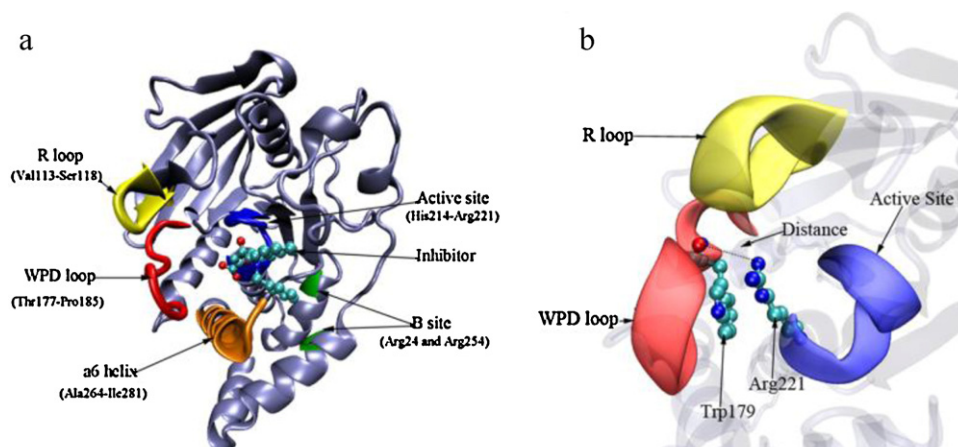


Fig. 1. (a) The three-dimensional structure of PTP-1B with highlight regions. (b) The distance of the backbone carbonyl oxygen of Trp179 and the nitrogen of the guanidinium moiety of Arg221 in PTP-1B.

Excellent work has been conducted on this topic over the past two decades. Many compounds have been studied and have been proven to be potential inhibitors. Vanadate [19–21], for example, was the first and most extensively investigated PTP1B inhibitor. Selectivity is a challenging issue in the design of PTP-1B inhibitors. In 1997, Zhang and his colleagues discovered a second binding active site near the conserved primary active site [15]. This binding site is not as conserved and can be exploited to design PTP-1B inhibitors with high selectivities. Since then, numerous bidentate compounds have been studied and have been proven to be potential and selective PTP-1B inhibitors [17,22–31]. However, these compounds contain negatively charged nonhydrolyzable phosphotyrosine (pTyr) mimetics and have poor membrane permeability, which results in their inability to readily enter the cell. Consequently, the identification of compounds with good bioavailability is still a major challenge in this field.

Recently, aryl diketoacids have been reported by Liu et al. to be potential noncompetitive, active site-directed and selective PTP-1B inhibitors [32]. The significance of these compounds stems from the dimeric aryl diketoacid lacking any formal charge, being cell-permeable and also exhibiting PTP-1B inhibitory activity. These properties may solve the bioavailability problem in pharmaceutical applications. Regrettably, little research has been conducted on these PTP-1B inhibitors. This work is intended to fill this gap through analysis of the interaction models of these compounds via molecular dynamics (MD) simulations. Hydrogen bonds, binding energies and conformation changes of the WPD loop are analyzed in this work.

2. Methods

2.1. Simulation models

Six aryl diketoacid compounds are adopted as the object of study (see Table 1). Three of them (LZP4, LZP38 and LZP25) are monomeric aryl diketoacid compounds that exhibit inhibitory activity for PTP1B. Three corresponding dimers (LZP6, LZP38 and LZP40) linked with the piperazine show an improvement in the inhibitory activity [32]. The atom label follows the nomenclature of the standard GROMACS96 43a2 force field. The geometry of six aryl diketoacid compounds is optimized using the Gaussian03 [33] program at the level of B3LYP/6-31G(d) [17,27].

The crystal structures of PTP-1B-LZP25 Complex (PDB ID: 3EB1 [32]) and LZP6-PTP-1B Complex (PDB ID: 3EAX [32]) were

downloaded from the Protein Data Bank [34]. Because the crystal structure of 3EAX (LZP6-PTP-1B) is a high-resolution (1.9 Å) X-ray structure, we selected it for the generation of the initial models. Crystallographic water molecules and ligands in 3EAX were removed. Six aryl diketoacid compounds were subsequently docked into the binding pocket using the AutoDock4.2 program [35]. The binding model with lowest binding free energy for each inhibitor is selected as the best model. The binding positions for the six inhibitors are listed in Supporting information (Fig. S1). The best models generated here served as initial structures for subsequent molecular dynamics simulations.

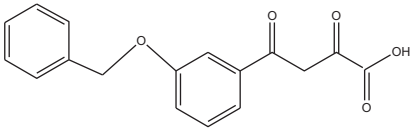
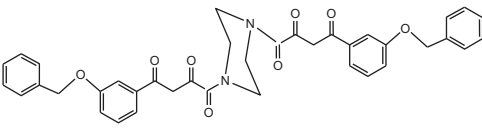
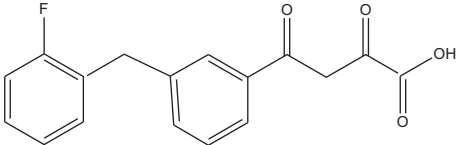
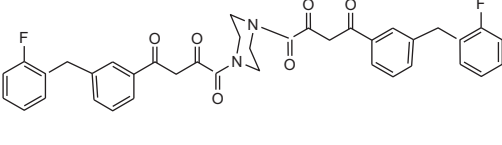
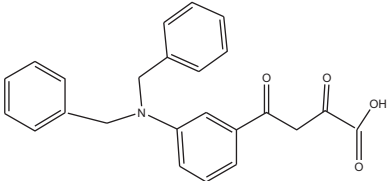
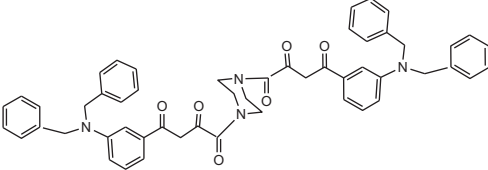
2.2. Molecular dynamics simulations

The molecular dynamics (MD) simulations were performed using the GROMACS program (version 4.0.5) with the GROMACS96 43a2 force field [36]. The molecular topology file and the force-field parameters for the inhibitors were generated by the program PRODRG online [37]. PRODRG is an automated topology generation tool that has been widely used in the study of protein–ligand systems [29,31,38,39]. The charges of the inhibitors generated by this server have also been validated in similar compounds [29]. The generated charges of six inhibitors are listed in Supporting information (Tables SI–SII). Each model was solvated with explicit simple point charge (SPC) water embedded in a $70 \text{ Å} \times 70 \text{ Å} \times 70 \text{ Å}$ box. The total charge of the system was -1 . To achieve charge neutrality in the system, one sodium ion was added in place of one water molecule in the box.

The systems were then subjected to a steepest-descent energy minimization until they reached a tolerance of 1000 kJ/mol. All bonds that contained hydrogen bonds were constrained using the LINCS algorithm [40]. The Nose–Hoover and Parrinello–Rahman algorithms were used for the temperature and pressure coupling. The value of the isothermal compressibility was set to $4.5 \times 10^{-5} \text{ bar}^{-1}$ for water simulations. The electrostatic interaction energy was calculated using the particle-mesh Ewald (PME) algorithm [41], with an interpolation order of 4 and a grid spacing of 1.2 Å. The cut-off of van der Waals (vdW) interaction was 10 Å.

Finally, a 20 ns MD simulation was performed for each system under a temperature of 300 K and a pressure of 1 bar with a coupling time constant of 2.0 ps. The time step was 2 fs, and the trajectories were collected every 1 ps. The last 5 ns were used for further analyses.

Table 1
Six mono and dimeric aryl diketoacid PTP-1B inhibitors.

Monomer	Dimers
 <p>LZP4</p>	 <p>LZP6</p>
 <p>LZP38</p>	 <p>LZP37</p>
 <p>LZP25</p>	 <p>LZP40</p>

2.3. Contributions of the van der Waals interaction energy and the electrostatic interaction energy

The trajectories of the last 5 ns were adopted to analyze the contributions of the van der Waals interaction energy and the electrostatic interaction energy. As shown in Eq. (1), the total potential energy of the system was decomposed into four terms: the intra-molecular interaction of the inhibitor ($E_{\text{inhibitor-inhibitor}}$), the interaction between the residues ($E_{\text{residue-residue}}$), the interaction of each inhibitor-residue pair ($E_{\text{inhibitor-residue}}$), and other interactions (E_{others}).

$$E_{\text{total}} = E_{\text{inhibitor-inhibitor}} + E_{\text{residue-residue}} + E_{\text{inhibitor-residue}} + E_{\text{others}} \quad (1)$$

$$E_{\text{inhibitor-residue}} = E_{\text{vdW}} + E_{\text{ele}} \quad (2)$$

We focused only on the interaction of each inhibitor-residue pair ($E_{\text{inhibitor-residue}}$), which included two terms: the vdW contribution (E_{vdW}) and the electrostatic contribution (E_{ele}). These contributions are non-bonded interactions between residues and one inhibitor (Eq. (2)). A cutoff of 10 Å for the vdW interactions was adopted.

2.4. Stability of hydrogen bonds

The hydrogen-bond existence map between the inhibitor and the residues was calculated using the trajectories of the last 5 ns. We noticed that the hydrogen-bond existence map did not provide a good quantitative description of the stability of the hydrogen bonds. Consequently, a simple function was defined to describe the stability of the hydrogen bonds: the frequency of existence (FE). As shown in Eq. (3), the frequency of existence (FE) is defined as follows:

$$\text{FE} = \frac{N_{\text{existence}}}{N_{\text{collected frames}}} \times 100\% \quad (3)$$

In Eq. (3), $N_{\text{existence}}$ is the amount of frames that contain targeted hydrogen bonds, and $N_{\text{collected frames}}$ is the number of collected

frames. In this work, we collected one frame from the trajectories every 20 ps. The FE of each hydrogen bond was calculated in terms of a percentage that varied from 1% to 100%, where a percentage of 100 indicates that the hydrogen bond is highly stable and a percentage of 1 indicates an unstable hydrogen bond.

3. Results and discussion

3.1. Molecular dynamics trajectory analysis

The stabilities of the trajectories for the PTP-1B complex systems are reflected in the total energies and in the RMSD of certain atoms in the initial structure. As shown in Fig. 2, the total energy oscillated around the average energy. The RMSD of the systems appeared to exhibit no prominent changes after 2.5 ns (except LZP37-PTP-1B, which showed no changes after 7.5 ns). These results indicate the equilibrium of the six systems at 300 K and at a pressure of 1 atm. Analyses of the two graphs demonstrated that the trajectories are sufficiently stable and that the production simulation is reliable.

3.2. WPD loop conformational changes

The movement of the WPD loop is a major conformational change that is essential to substrate binding. As described in previous studies [42], the WPD loop conformation is referred to as being in the “open” or the “closed” state, which is characterized by the distance between the backbone carbonyl oxygen of Trp179 and the nitrogen of the guanidinium moiety of Arg221 (see Fig. 1). If the distance covers a range of 2.35–2.99 Å, the WPD loop conformation should be in the closed state. If the distance covers a range of 4.15–5.22 Å, it should be the open state [43]. To confirm the conformation of the WPD loop, we calculated the average distances of six aryl diketoacid PTP-1B complexes, and the results are listed in Table 2.

Interestingly, the three monomeric aryl diketoacid PTP-1B complexes were all found to be in the transition state between the open and closed states, i.e., semi-open and semi-closed. However, the

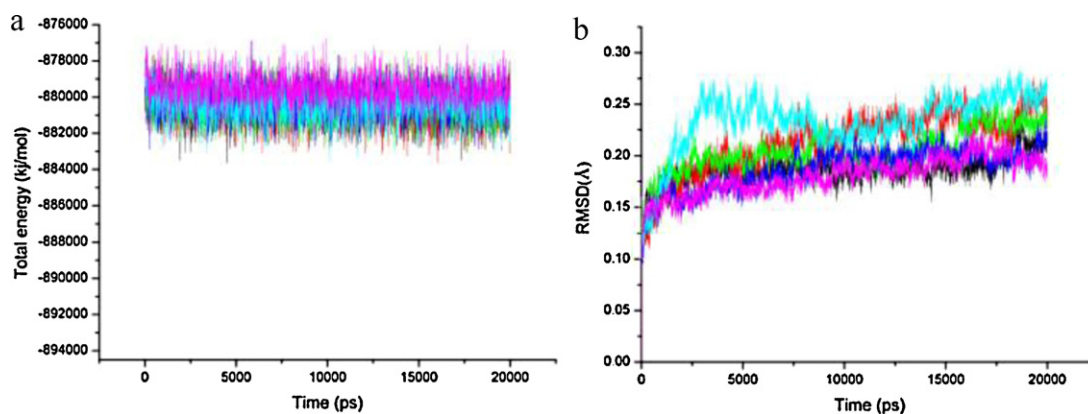


Fig. 2. Total energies (a) and RMSD (b) at each ps for six aryl diketoacid PTP-1B complexes along the MD trajectories. The curves for the PTP-1B-LZP4, PTP-1B-LZP38, PTP-1B-LZP25, PTP-1B-LZP6, PTP-1B-LZP37 and PTP-1B-LZP40 systems are colored black, red, green, blue, cyan, and magenta respectively. (For interpretation of the references to color in this figure legend, the reader is referred to the web version of this article.)

Table 2

The average distance (Å) of the backbone carbonyl oxygen of Trp179 and the nitrogen of the guanidinium moiety of Arg221.

Mono complexes		Dimeric complexes	
LZP4-PTP-1B	3.68	LZP6-PTP-1B	3.94
LZP38-PTP-1B	3.23	LZP37-PTP-1B	5.93
LZP25-PTP-1B	3.22	LZP40-PTP-1B	4.86

three corresponding dimers were found to be in the open state. The average distances of LZP38-PTP-1B (3.23 Å) and LZP25-PTP-1B (3.22 Å) are similar to but lower than that of LZP4-PTP-1B (3.68 Å). Liu et al. have reported that 3EB1 (LZP25-PTP-1B) adopts an open conformation (4.87 Å) [32]. To further investigate this matter, we also selected the crystal structure 3EB1 (LZP25-PTP-1B) as the initial structure, which was also adopted in the work of Liu et al. Then, a molecular simulation process (see Section 2) was performed in a manner similar to that used for other models. However, the average distance of the WPD loop conformation (3.11 Å) was very close to the value obtained in our simulation (3.22 Å). However, the WPD loop of LZP40-PTP-1B (4.86 Å) was in the completely open state and the average distance of PTP-1B-LZP37 was 5.93 Å, which is larger than that in the standard open state. The WPD loop conformation of LZP6-PTP-1B is somewhat different (3.94 Å) but is in an almost-open state.

Based on kinetic analyses, we know that the inhibition of LZP25 and LZP6 on PTP-1B may stabilize the inactive conformation of the WPD loop [32]. Hence, two questions arise: the first question is why the WPD loop prefers to adopt a non-closed state for the monomer and an open state for dimeric aryl diketoacid PTP-1B complexes,

even though both of them exhibit inhibitory activity for PTP-1B; the second question is whether their binding model is the same. To answer these two questions, the interactions between the aryl diketoacids and PTP-1B were further analyzed.

3.3. Hydrogen-bond analysis

The hydrogen-bonding interactions between PTP-1B and the six aryl diketoacids were investigated on the basis of the trajectories of the last 5 ns. Detailed information for the hydrogen bonds in the six aryl diketoacids with PTP-1B is shown in Table 3 and Fig. 3. The numbers of hydrogen bonds and the hydrogen-bond existence map are shown in Supporting information (Figs. S2 and S3).

As shown in Table 3 and Fig. 3, three monomeric aryl diketoacids all form stable hydrogen bonds with Arg221 and Ala217 of the active site. In addition, LZP4 also forms hydrogen bonds with Asn111, and LZP25 forms hydrogen bonds with Ser216. The analysis of the hydrogen-bond existence map shows that the hydrogen bonds are not stable (FE = 8%). The hydrogen bonds of LZP25 and Ser216 have also been detected in previous crystallographic studies [32].

The dominant hydrogen-bond regions and the stability of the dimeric aryl diketoacids differ from those of their corresponding monomeric aryl diketoacids. As shown in Table 3, four hydrogen bonds between LZP6 and PTP-1B are less stable than the other hydrogen bonds between these components. The main hydrogen-bond region is around the R-loop (Lys120 and Lys116) and the α 6-helix (Gln262). As reported in the crystallographic study [32], Lys116 forms one hydrogen bond with LZP6, which is mediated by a water molecule. In our simulation, a water molecule

Table 3

List of detailed information of hydrogen bonds formed between six aryl diketoacid compounds and PTP-1B.

Inhibitor		PTP-1B			Inhibitor		PTP-1B		
Monomer	Atom	Residue	Atom	FE	Dimer	Atom	Residue	Atom	FE
LZP4	O5	Arg221	N	81%	LZP6	O55	Lys120	NZ	43%
	O6	Ala 217	N	59%		O49	Lys120	NZ	14%
	O6	Asn 111	ND2	30%		O50	Lys116	NZ	12%
	O5	Asn 111	ND2	21%		O4	Gln262	NE2	20%
LZP38	O6	Arg221	N	81%	LZP37	O6	Phe182	N	100%
	O5	Ala 217	N	83%		O5	Arg221	N	33%
LZP25	O4	Arg221	N	50%	LZP40	OAB	Gly183	N	9%
	O7	Arg221	N	41%		OBL	Gly183	N	13%
	O5	Ala 217	N	70%		OBO	Arg268	N	23%
	O6	Ser216	N	8%					

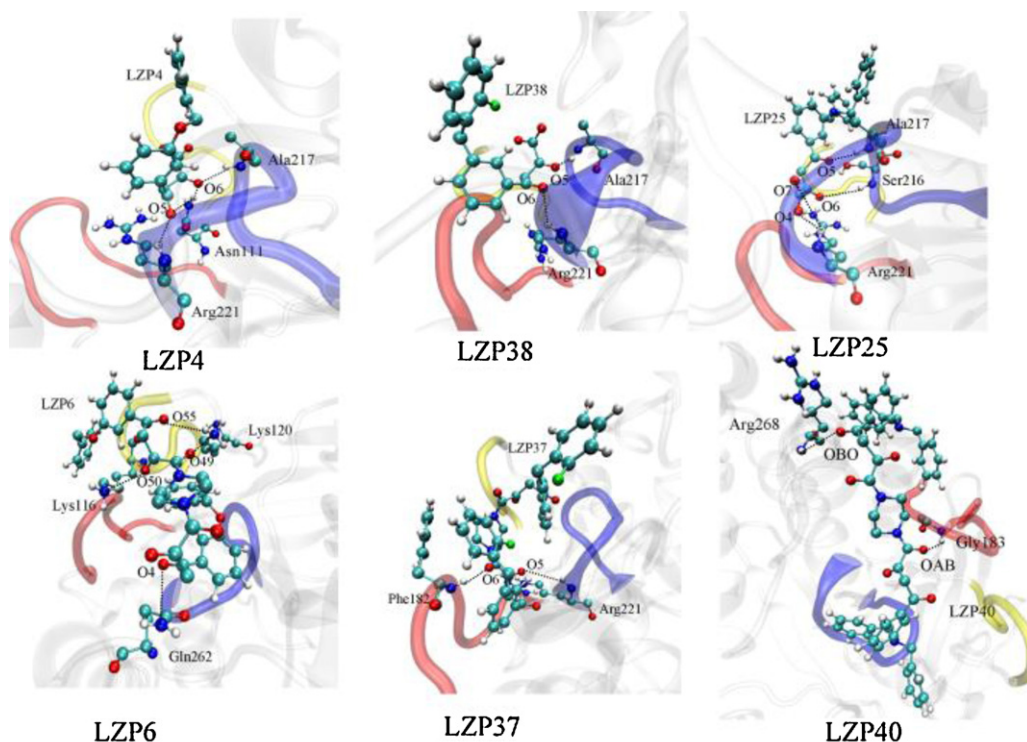


Fig. 3. The schematic diagram of the hydrogen bond (dash line) formed between six aryl diketoacids and PTP-1B.

acting as a medium between LZP6 and Lys116 can also be observed (Supporting information, Fig. S4); however, it is not as stable as expected (FE = 12%). In the case of PTP-1B-LZP37, the N atom of Phe182 of the WPD loop forms a stable hydrogen bond with LZP37. The N atom of Arg221 of the active site is involved with a less-stable hydrogen bond (FE = 33%). In the PTP-1B-LZP40, two hydrogen bonds formed with Gly183 and Arg268 are unstable over the time span of the simulation.

In general, a bidentate hydrogen bond will form between the oxyanion of the ligand and the guanidinium group of Arg221, whereas pTyr or an optimal nonhydrolyzable pTyr mimetic is bound to the active site [15,28,44]. This bidentate hydrogen bond appears to serve as a trigger that can initiate a series of interactions between Arg221 and the side chains of the invariant Glu115 and Trp179 in the WPD loop. These interactions are essential for the WPD loop to remain in the closed conformation [45–47]. However,

the six aryl diketoacids do not form the bidentate hydrogen bond with the guanidinium of Arg221, which results in the WPD loop of their complexes preferring to adopt the non-closed conformation. LZP37 and LZP40 directly form the hydrogen bond with residues of the WPD loop, which effectively restricts the movement of the WPD loop. This restriction may explain why LZP37 and LZP40 stabilize in the open conformation. Simultaneously, the distance differences in the six complexes indicate that steric clash is not the major factor that determines whether the WPD loop exists in the open or closed conformation.

3.4. The interaction between PTP-1B and aryl diketoacids

The mode of the interaction between the aryl diketoacids and the target protein PTP-1B was further studied on the basis of binding energies. The binding-energy contributions of the vdW and

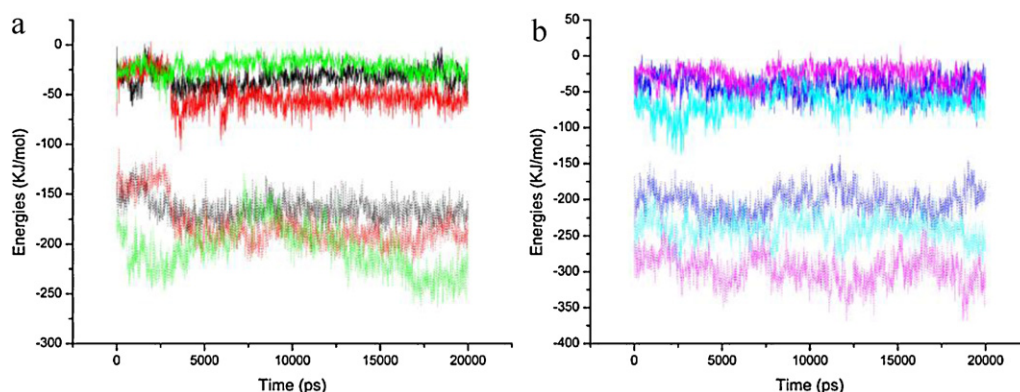


Fig. 4. (a) The short-range electrostatic energies (solid line) and van der Waals energies (dash line) for monomeric aryl diketoacids and PTP-1B. (b) The short-range electrostatic energies (solid line) and van der Waals energies (dash line) for dimeric aryl diketoacids and PTP-1B. The curves for the PTP-1B-LZP4, PTP-1B-LZP38, PTP-1B-LZP25, PTP-1B-LZP6, PTP-1B-LZP37 and PTP-1B-LZP40 systems are colored black, red, green, blue, cyan, and magenta respectively. (For interpretation of the references to color in this figure legend, the reader is referred to the web version of this article.)

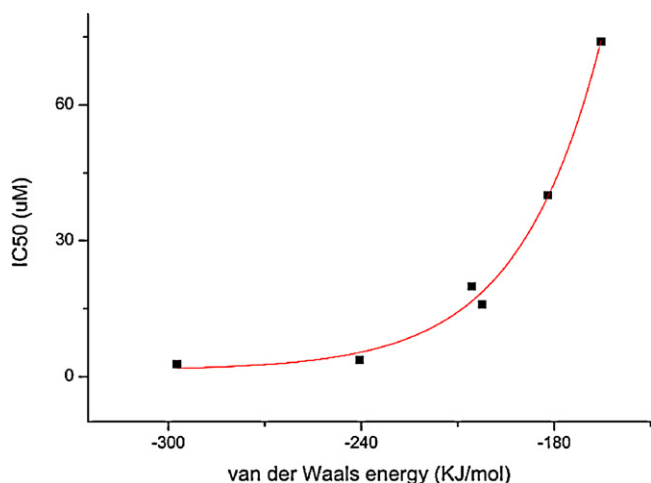


Fig. 5. The relationship between IC50 values and van der Waals interaction energies of each compound.

short-range electrostatic energies have also been calculated and are discussed.

Obviously, in Fig. 4, the vdW energies are stronger than the corresponding short-range electrostatic energies in the six aryl diketoacid PTP-1B complexes. Therefore, the vdW interaction should play a role more important than that of the short-range electrostatic interaction. Notably, the relative order of the vdW interaction energies is consistent with their half-maximal inhibitory concentration (IC50) determined in experimental studies [32]. The relationship between the IC50 values and the corresponding vdW interaction energies were fitted, and the results are shown in Fig. 5. The two values exhibit an approximate exponential relationship, and the exponential formula is $y = a \times \exp(-x/b) + c$, where x is the absolute value of the vdW interaction energy and y is the IC50 value. The fitted parameters are $a = 4.5 \times 10^4$, $b = 25.73$ and $c = 1.42$. This formula indicates that, with the increase of vdW interaction energies, the inhibitory activity of the inhibitor is gradually strengthened. The vdW interaction energies of the dimeric aryl diketoacid PTP-1B complexes are stronger than those of the corresponding monomeric aryl

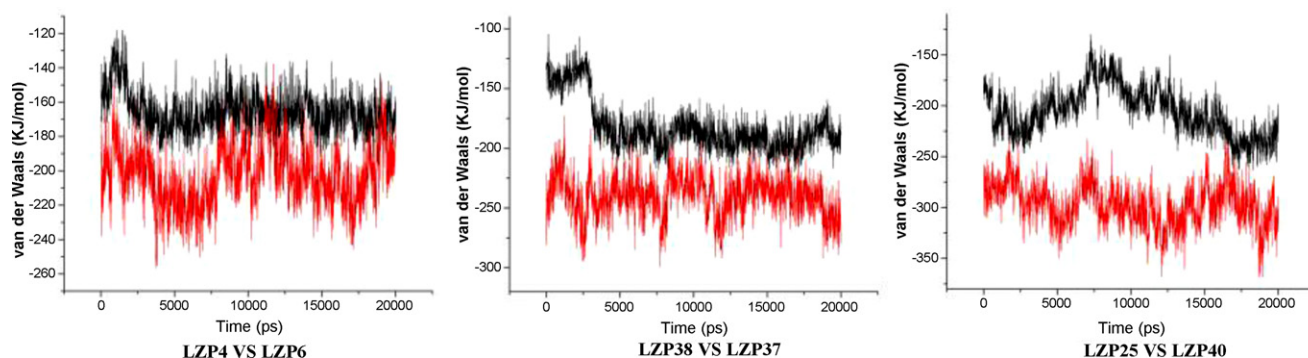


Fig. 6. Comparison of van der Waals interaction energies between monomeric and dimeric aryl diketoacid PTP-1B complexes, the curve of mono and corresponding dimers are colored by black and red respectively. (For interpretation of the references to color in this figure legend, the reader is referred to the web version of this article.)

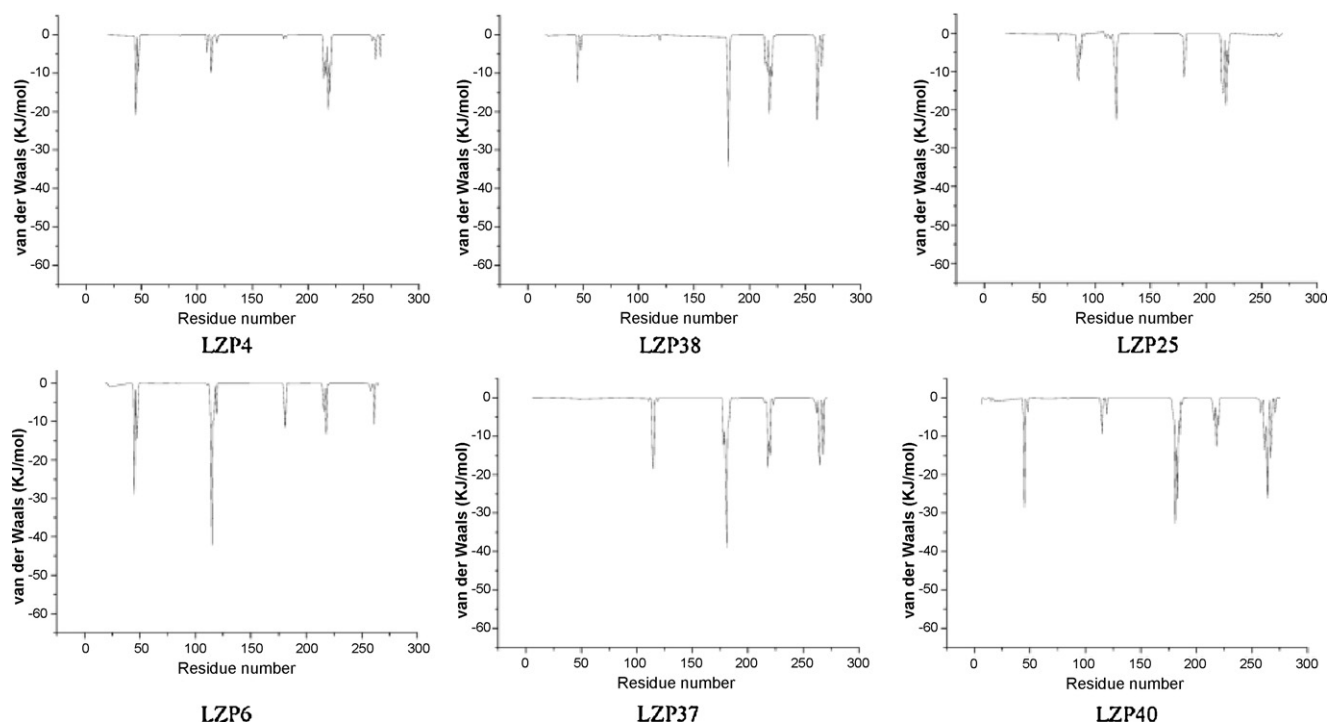


Fig. 7. van der Waals interaction energy contributions of residues to six aryl diketoacid PTP-1B complexes.

Table 4
Residues involved in cooperative effects of the van der Waals interaction and hydrogen bonds.

Monomer	van der Waals Primary site	Hydrogen bond	Dimer	van der Waals Primary site	Hydrogen bond
LZP4	Active site (His214–Arg221)	Ala217, Arg221	LZP6	R loop (Val113–Ser118) Leu119 and Lys120	Lys120
LZP38	Active site (His214–Arg221)	Ala217, Arg221	LZP37	WPD loop (Thr177–Pro185)	Phe182
LZP25	Active site (His214–Arg221)	Ala217, Arg221	LZP40	WPD loop (Thr177–Pro185)	Gly183

diketoacid PTP-1B complexes (Fig. 6). Therefore, the dimeric aryl diketoacids show an improved PTP-1B inhibitory activity relative to that of the corresponding monomers. The above analyses provide a deeper understanding of the reported experimental findings [32], where dimeric aryl diketoacids have been reported to show higher PTP-1B inhibitory activity than the monomers. Furthermore, we suggest that the effective increase in the vdW interaction improves the inhibitory activity of aryl diketoacids for targeting PTP-1B. At this point, experimental investigations were still needed. Hence, strategies for improving the vdW interactions during the design of inhibitors will be further elaborated in Section 3.5.

3.5. Cooperative vdW interaction and hydrogen bond

Contributions of vdW interaction energies to each residue were analyzed using the six aryl diketoacid PTP-1B complexes (see Fig. 7). For the three mono aryl diketoacid PTP-1B complexes, His214 to Arg221 of the active site show the primary and positive contributions to the vdW interaction. For the three dimeric aryl diketoacid PTP-1B complexes, the dominant contribution originates from the WPD loop or the R-loop. The adoption of different binding models by the two types of complexes is reasonable, even if they all promote a non-closed conformation of the WPD loop. Therefore, the targeting regions of these compounds differ significantly. For mono aryl diketoacids, the vdW interaction with the active site should be enhanced, whereas, for dimeric aryl diketoacids, the vdW interaction to the WPD loop or the R loop should be enhanced.

When the vdW interaction and the hydrogen-bond regions were compared, a cooperative effect was found between them. The residues that involve cooperative effects are summarized and shown in Table 4. In the monomeric aryl diketoacid-bound complexes, Arg221 and Ala217 of the active site are also involved in the formation of a stable hydrogen bond. In the dimeric aryl diketoacid-bound complexes, the R-loop (Glu115 to Lys118), Leu119 and Lys120 show the main and positive contributions to the vdW interaction in LZP6-PTP-1B. Lys120 is also involved in the formation of a stable hydrogen bond. In LZP37-PTP-1B and LZP40-PTP-1B, Trp178 to Val185 of the WPD loop make the primary and positive contributions to the vdW interaction. Phe182 and Gly183 are found to form the hydrogen bond with LZP37 and LZP40, respectively. Hence, the vdW interaction cooperates with the hydrogen-bond interactions through the six aryl diketoacid PTP-1B complexes.

The cooperative effects in several inhibitor binding processes have been discussed elsewhere [17,48,49]. In this case, the vdW interaction and the hydrogen-bond interaction combine to form cooperative effects when the aryl diketoacid is bound with the PTP-1B. To improve the vdW interaction energy, the design of more stable hydrogen bonds in the active site (for mono aryl diketoacids) or the WPD loop and R-loop regions (dimeric aryl diketoacids) is a potential solution.

4. Conclusion

PTP-1B is a major negative regulator in both insulin and leptin signaling. It has been observed to serve as an outstanding target

for the treatment of some human diseases. Three monomeric aryl diketoacids and their corresponding amide-linked dimeric PTP-1B complexes were investigated on the basis of MD simulations. The conformation of the WPD loop adopts the inactive and non-closed state in the six investigated aryl diketoacid PTP-1B complexes. Through hydrogen bond analyses, the bidentate hydrogen bond between the guanidinium of Arg221 and the oxyanion of the six aryl diketoacids is not formed, and the WPD loop closure cannot be sufficiently triggered. Binding-energy analyses show that the vdW interaction plays a more significant role than short-range electrostatic interactions. An exponential relationship between the IC₅₀ values and the vdW interaction energies was obtained, which may explain why the dimeric aryl diketoacids show high inhibitory activity for PTP-1B. Our comparative study revealed that monomeric and dimeric aryl diketoacids have absolutely different binding modes when targeting the PTP-1B. The active site of PTP-1B is the primary target site for the monomeric aryl diketoacids. The R loop or WPD loop of PTP-1B is the primary target site for dimeric aryl diketoacids. The vdW interaction and the hydrogen-bond interactions exhibit a cooperative relationship when the aryl diketoacid is bound with the PTP-1B. We hope that these findings will provide a novel strategy for the design of aryl diketoacids as efficient drugs for the treatment of treat cancer, diabetes and obesity.

Acknowledgments

This work was supported by the National Natural Science Foundation of China (No. 91127014), the Natural Science Foundation of Shandong Province of China (No. ZR2010BZ005) and the Independent Innovation Foundation of Shandong University (2010TS015). It was also supported by the Virtual Laboratory for Computational Chemistry, the Supercomputing Center of Chinese Academy of Science and the Shandong University High Performance Computing Center.

Appendix A. Supplementary data

Supplementary data associated with this article can be found, in the online version, at <http://dx.doi.org/10.1016/j.jmglm.2012.06.011>.

References

- [1] A. Alonso, J. Sasin, N. Bottini, I. Friedberg, I. Friedberg, A. Osterman, A. Godzik, T. Hunter, J. Dixon, T. Mustelin, Protein tyrosine phosphatases in the human genome, *Cell* 117 (2004) 699–711.
- [2] T. Hunter, Signaling—2000 and beyond, *Cell* 100 (2000) 113–127.
- [3] N.K. Tonks, B.G. Neel, From form to function: signaling by protein tyrosine phosphatases, *Cell* 87 (1996) 365–368.
- [4] L. Li, J.E. Dixon, Form, function, and regulation of protein tyrosine phosphatases and their involvement in human diseases, *Seminars in Immunology* 12 (2000) 75–84.
- [5] W.S. Cook, R.H. Unger, Protein tyrosine phosphatase 1B: a potential leptin resistance factor of obesity, *Developmental Cell* 2 (2002) 385–387.

- [6] E. Asante Appiah, B.P. Kennedy, Protein tyrosine phosphatases: the quest for negative regulators of insulin action, *American Journal of Physiology – Endocrinology and Metabolism* 284 (2003) E663–E670.
- [7] M. Elchebly, P. Payette, E. Michaliszyn, W. Cromlish, S. Collins, A.L. Loy, D. Normandin, A. Cheng, J. Himms-Hagen, C.C. Chan, C. Ramachandran, M.J. Gresser, M.L. Tremblay, B.P. Kennedy, Increased insulin sensitivity and obesity resistance in mice lacking the protein tyrosine phosphatase-1B gene, *Science* 283 (1999) 1544–1548.
- [8] L.D. Klamman, O. Boss, O.D. Peroni, J.K. Kim, J.L. Martino, J.M. Zabolotny, N. Moghal, M. Lubkin, Y.B. Kim, A.H. Sharpe, A. Stricker-Krongrad, G.I. Shulman, B.G. Neel, B.B. Kahn, Increased energy expenditure, decreased adiposity, and tissue-specific insulin sensitivity in protein-tyrosine phosphatase 1B-deficient mice, *Molecular and Cellular Biology* 20 (2000) 5479–5489.
- [9] T.O. Johnson, J. Ermoloeff, M.R. Jirousek, Protein tyrosine phosphatase 1B inhibitors for diabetes, *Nature Reviews Drug Discovery* 1 (2002) 696–709.
- [10] D. Popov, Novel protein tyrosine phosphatase 1B inhibitors: interaction requirements for improved intracellular efficacy in type 2 diabetes mellitus and obesity control, *Biochemical and Biophysical Research Communications* 410 (2011) 377–381.
- [11] S.C. Yip, S. Saha, J. Chernoff, PTP1B: a double agent in metabolism and oncogenesis, *Trends in Biochemical Sciences* 35 (2010) 442–449.
- [12] S. Zhang, Z.Y. Zhang, PTP1B as a drug target: recent developments in PTP1B inhibitor discovery, *Drug Discovery Today* 12 (2007) 373–381.
- [13] K.L. Guan, R.S. Haun, S.J. Watson, R.L. Geahlen, J.E. Dixon, Cloning and expression of a protein-tyrosine-phosphatase, *Proceedings of the National Academy Sciences of the United States of America* 87 (1990) 1501–1505.
- [14] K.M. Picha, S.S. Patel, S. Mandiyan, J. Koehn, L.P. Wengle, The role of the C-terminal domain of protein tyrosine phosphatase-1B in phosphatase activity and substrate binding, *Journal of Biological Chemistry* 282 (2007) 2911–2917.
- [15] Y.A. Puius, Y. Zhao, M. Sullivan, D.S. Lawrence, S.C. Almo, Z.Y. Zhang, Identification of a second aryl phosphate-binding site in protein-tyrosine phosphatase 1B: a paradigm for inhibitor design, *Proceedings of the National Academy Sciences of the United States of America* 94 (1997) 13420–13425.
- [16] A.P. Combs, E.W. Yue, M. Bower, P.J. Ala, B. Wayland, B. Douthy, A. Takvorian, P. Polam, Z. Wasserman, W. Zhu, M.L. Crawley, J. Pruitt, R. Sparks, B. Glass, D. Modi, E. McLaughlin, L. Bostrom, M. Li, L. Galya, K. Blom, M. Hillman, L. Gonneville, B.G. Reid, M. Wei, M. Becker-Pasha, R. Klaber, H. Huber, Y. Li, G. Hollis, T.C. Burn, R. Wynn, P. Liu, B. Metcalf, Structure-based design and structure-based design and discovery of protein tyrosine phosphatase inhibitors incorporating novel isothiazolidinone heterocyclic phosphotyrosine mimetics, *Journal of Medical Chemistry* 48 (2005) 6544–6548.
- [17] R. Kumar, R.N. Shinde, D. Ajay, M.E. Sobhia, Probing interaction requirements in PTP1B inhibitors: a comparative molecular dynamics study, *Journal of Chemical Information and Modeling* 50 (2010) 1147–1158.
- [18] R. Ottanà, R. Maccari, R. Ciurleo, P. Paoli, M. Jacomelli, G. Manao, G. Camici, C. Laggner, T. Langer, 5-Arylidene-2-phenylimino-4-thiazolidinones as PTP1B and LMW-PTP inhibitors, *Bioorganic & Medicinal Chemistry* 17 (2009) 1928–1937.
- [19] A.P. Seale, L.A. de Jesus, S.Y. Kim, Y.H. Choi, H.B. Lim, C.S. Hwang, Y.S. Kim, Development of an automated protein-tyrosine phosphatase 1B inhibition assay and the screening of putative insulin-enhancing vanadium(IV) and zinc(II) complexes, *Biotechnology Letters* 27 (2005) 221–225.
- [20] K.H. Thompson, C. Orvig, Vanadium in diabetes: 100 years from Phase 0 to Phase I, *Journal of Inorganic Biochemistry* 100 (2006) 1925–1935.
- [21] C. Yuan, L. Lu, Y. Wu, Z. Liu, M. Guo, S. Xing, X. Fu, M. Zhu, Synthesis, characterization, and protein tyrosine phosphatases inhibition activities of oxovanadium(IV) complexes with Schiff base and polypyridyl derivatives, *Journal of Inorganic Biochemistry* 104 (2010) 978–986.
- [22] S.R. Klopfenstein, A.G. Evdokimov, A.O. Colson, N.T. Fairweather, J.J. Neuman, M.B. Maier, J.L. Gray, G.S. Gerwe, G.E. Stake, B.W. Howard, J.A. Farmer, M.E. Pokross, T.R. Downs, B. Kasibhatla, K.G. Peters, 1,2,3,4-Tetrahydroisquinolinyl sulfamic acids as phosphatase PTP1B inhibitors, *Bioorganic and Medical Chemistry Letters* 16 (2006) 1574–1578.
- [23] A.F. Moretto, S.J. Kirincich, W.X. Xu, M.J. Smith, Z.K. Wan, D.P. Wilson, B.C. Follows, E. Binnun, D. Joseph McCarthy, K. Foreman, D.V. Erbe, Y.L. Zhang, S.K. Tam, S.Y. Tam, J. Lee, Bicyclic and tricyclic thiophenes as protein tyrosine phosphatase 1B inhibitors, *Bioorganic and Medical Chemistry* 14 (2006) 2162–2177.
- [24] Z.H. Pei, X.F. Li, G. Liu, C. Abad Zapatero, T. Lubben, T.Y. Zhang, S.J. Ballaron, C.W. Hutchins, J.M. Trevillyan, M.R. Jirousek, Discovery and SAR of novel, potent and selective protein tyrosine phosphatase 1B inhibitors, *Bioorganic and Medical Chemistry Letters* 13 (2003) 3129–3132.
- [25] B.G. Szczepankiewicz, G. Liu, P.J. Hajduk, C. Abad Zapatero, Z.H. Pei, Z.L. Xin, T.H. Lubben, J.M. Trevillyan, M.A. Stashko, S.J. Ballaron, H. Liang, F. Huang, C.W. Hutchins, S.W. Fesik, M.R. Jirousek, Discovery of a potent, selective protein tyrosine phosphatase 1B inhibitor using a linked-fragment strategy, *Journal of the American Chemical Society* 125 (2003) 4087–4096.
- [26] G. Liu, Z.L. Xin, Z.G. Pei, P.J. Hajduk, C. Abad-Zapatero, C.W. Hutchins, H.Y. Zhao, T.H. Lubben, S.J. Ballaron, D.L. Haasch, W. Kaszubska, C.M. Rondinone, J.M. Trevillyan, M.R. Jirousek, Fragment screening and assembly: a highly efficient approach to a selective and cell active protein tyrosine phosphatase 1B inhibitor, *Journal of Medical Chemistry* 46 (2003) 4232–4235.
- [27] F. Lei, Z. Huai, C. Wei, J. Mingjun, Studies of the mechanism of selectivity of protein tyrosine phosphatase 1B (PTP1B) bidentate inhibitors using molecular dynamics simulations and free energy calculations, *Journal of Chemical Information and Modeling* 48 (2008) 2030–2041.
- [28] J.P. Sun, A.A. Fedorov, S.Y. Lee, X.L. Guo, K. Shen, D.S. Lawrence, S.C. Almo, Z.Y. Zhang, Crystal structure of PTP1B complexed with a potent and selective bidentate inhibitor, *Journal of Biological Chemistry* 278 (2003) 12406–12414.
- [29] J.F. Wang, K. Gong, D.Q. Wei, Y.X. Li, K.C. Chou, Molecular dynamics studies on the interactions of PTP1B with inhibitors: from the first phosphate-binding site to the second one, *Protein Engineering, Design and Selection* 22 (2009) 349–355.
- [30] X. Zhang, X. Li, R. Wang, Interpretation of the binding affinities of PTP1B inhibitors with the MM-CB/SA method and the X-score scoring function, *Journal of Chemical Information and Modeling* 49 (2009) 1033–1048.
- [31] G.X. Liu, J.Z. Tan, C.Y. Niu, J.H. Shen, X.M. Luo, X. Shen, K.X. Chen, H.L. Jiang, Molecular dynamics simulations of interaction between protein-tyrosine phosphatase 1B and a bidentate inhibitor, *Acta Pharmacologica Sinica* 27 (2006) 100–110.
- [32] S. Liu, L.F. Zeng, L. Wu, X. Yu, T. Xue, A.M. Gunawan, Y.-Q. Long, Z.Y. Zhang, Targeting inactive enzyme conformation: aryl diketoacid derivatives as a new class of PTP1B inhibitors, *Journal of the American Chemical Society* 130 (2008) 17075–17084.
- [33] M.J. Frisch, G.W. Trucks, H.B. Schlegel, G.E. Scuseria, M.A. Robb, J.R. Cheeseman, J.A. Montgomery, Jr., T. Vreven, K.N. Kudin, J.C. Burant, J.M. Millam, S.S. Iyengar, J. Tomasi, V. Barone, B. Mennucci, M. Cossi, G. Scalmani, N. Rega, G.A. Petersson, H. Nakatsuji, M. Hada, M. Ehara, K. Toyota, R. Fukuda, J. Hasegawa, M. Ishida, T. Nakajima, Y. Honda, O. Kitao, H. Nakai, M. Klene, X. Li, J.E. Knox, H.P. Hratchian, J.B. Cross, V. Bakken, C. Adamo, J. Jaramillo, R. Gomperts, R.E. Stratmann, O. Yazyev, A.J. Austin, R. Cammi, C. Pomelli, J.W. Ochterski, P.Y. Ayala, K. Morokuma, G.A. Voth, P. Salvador, J.J. Dannenberg, V.G. Zakrzewski, S. Dapprich, A.D. Daniels, M.C. Strain, O. Farkas, D.K. Malick, A.D. Rabuck, K. Raghavachari, J.B. Foresman, J.V. Ortiz, Q. Cui, A.G. Baboul, S. Clifford, J. Cioslowski, B.B. Stefanov, G. Liu, A. Liashenko, P. Piskorz, I. Komaromi, R.L. Martin, D.J. Fox, T. Keith, M.A. Al-Laham, C.Y. Peng, A. Nanayakkara, M. Challacombe, P.M.W. Gill, B. Johnson, W. Chen, M.W. Wong, C. Gonzalez, J.A. Pople, Gaussian 03, revision C.02., Gaussian Inc., Wallingford, 2004.
- [34] H.M. Berman, J. Westbrook, Z. Feng, G. Gilliland, T.N. Bhat, H. Weissig, I.N. Shindyalov, P.E. Bourne, The protein data bank, *Nucleic Acids Research* 28 (2000) 235–242.
- [35] G.M. Morris, D.S. Goodsell, R.S. Halliday, R. Huey, W.E. Hart, R.K. Belew, A.J. Olson, Automated docking using a Lamarckian genetic algorithm and an empirical binding free energy function, *Journal of Computational Chemistry* 19 (1998) 1639–1662.
- [36] H.J.C. Berendsen, D. van der Spoel, R. van Drunen, GROMACS: a message-passing parallel molecular dynamics implementation, *Computer Physics Communications* 91 (1995) 43–56.
- [37] D.M.F. Van Aalten, R. Bywater, J.B.C. Findlay, M. Hendlich, R.W.W. Hooft, G. Vriend, PRODRG, a program for generating molecular topologies and unique molecular descriptors from coordinates of small molecules, *Journal of Computer Aided Molecular Design* 10 (1996) 255–262.
- [38] J. Li, X. Zhu, C. Yang, R. Shi, Characterization of the binding of angiotensin II receptor blockers to human serum albumin using docking and molecular dynamics simulation, *Journal of Molecular Modeling* 16 (2010) 789–798.
- [39] M. Sharma, S. Khanna, G. Bulusu, A. Mitra, Comparative modeling of thioredoxin glutathione reductase from *Schistosoma mansoni*: a multifunctional target for antischistosomal therapy, *Journal of Molecular Graphics and Modeling* 27 (2009) 665–675.
- [40] B. Hess, H. Bekker, H.J.C. Berendsen, J.G.E.M. Fraaije, LINC: a linear constraint solver for molecular simulations, *Journal of Computational Chemistry* 18 (1997) 1463–1472.
- [41] T. Darden, D. York, L. Pedersen, Particle mesh Ewald: an $N \log(N)$ method for Ewald sums in large systems, *Journal of Chemical Physics* 98 (1993) 10089–10092.
- [42] S.C.L. Kamerlin, R. Rucker, S. Boresch, A targeted molecular dynamics study of WPD loop movement in PTP1B, *Biochemical and Biophysical Research Communications* 345 (2006) 1161–1166.
- [43] S.C. Lynn Kamerlin, R. Rucker, S. Boresch, A molecular dynamics study of WPD-loop flexibility in PTP1B, *Biochemical and Biophysical Research Communications* 356 (2007) 1011–1016.
- [44] Z. Jia, D. Barford, A. Flint, N. Tonks, Structural basis for phosphotyrosine peptide recognition by protein tyrosine phosphatase 1B, *Science* 268 (1995) 1754–1758.
- [45] Y.F. Keng, L. Wu, Z.Y. Zhang, Probing the function of the conserved tryptophan in the flexible loop of the *Yersinia* protein-tyrosine phosphatase, *European Journal of Biochemistry* 259 (1999) 809–814.
- [46] R.H. Hoff, A.C. Hengge, L. Wu, Y.F. Keng, Z.Y. Zhang, Effects on general acid catalysis from mutations of the invariant tryptophan and arginine residues in the protein tyrosine phosphatase from *Yersinia*, *Biochemistry—US* 39 (1999) 46–54.
- [47] Z.Y. Zhang, Mechanistic studies on protein tyrosine phosphatases, in: M. Kivie (Ed.), *Progress in Nucleic Acids Research*, vol. 73, Academic Press, 2003, pp. 171–220.
- [48] B.R.A. Persson, B. Jönsson, M. Lund, Enhanced protein steering: cooperative electrostatic and van der Waals forces in antigen-antibody complexes, *Journal of Physical Chemistry B* 113 (2009) 10459–10464.
- [49] B. Kuhn, J.E. Fuchs, M. Reutlinger, M. Stahl, N.R. Taylor, Rationalizing tight ligand binding through cooperative interaction networks, *Journal of Chemical Information and Modeling* 51 (2011) 3180–3198.